ELSEVIER

Journal of Chromatography A, 742 (1996) 55–68

JOURNAL OF CHROMATOGRAPHY A

Peak tailing and slow mass transfer kinetics in nonlinear chromatography

Torgny Fornstedt[a,b,1], Guoming Zhong[a,b], Georges Guiochon[a,b,*]

[a]*Department of Chemistry, University of Tennessee, Knoxville, TN 37996-1600, USA*

[b]*Division of Chemical and Analytical Sciences, Oak Ridge National Laboratory, Oak Ridge, TN 37831, USA*

Received 15 December 1995; revised 15 March 1996; accepted 15 March 1996

Abstract

Peak tailing has two main origins in chromatography: (i) heterogenous mass transfer kinetics, (ii) heterogenous thermodynamics with overloading of a nonlinear isotherm. The individual effects of each of these sources and the conditions under which they give rise to peak tailing are now well known. Often however, these different sources combine resulting in complex behavior. This situation is investigated in the case of an adsorbent whose surface is covered with two different types of adsorption sites. The first type of sites has a large specific surface area, a relatively weak adsorption energy and retention and fast mass transfer kinetics. The second type of sites covers a small proportion of the total surface area and has a strong retention and slow mass transfer kinetics. Tailing from different origins combine when the slow type of adsorption sites is operated under a certain degree of overloading, i.e., under nonlinear conditions. To model these phenomena, the transport–dispersive model was used with a modified solid film linear driving force model accounting for mass transfer kinetics on both types of sites. When the rate of mass transfer on the active sites is slow ($k_2 \leq 10$ min^{-1}), peak tailing of thermodynamic origin is negligible. When the kinetics is fast ($k_2 \geq 100$ min^{-1}), heterogenous thermodynamics is the source of peak tailing. In the intermediate region ($10 < k_2 < 100$ min^{-1}) peak tailing results from the combined effects of these sources, in an complicated interplay which is detailed in this study. The results of this study provide a most satisfactory explanation of the influence of the experimental conditions under which peak tailing arises in many analytical applications. This is the case, for example, of the chiral separations of small drug molecules on cellulase proteins immobilized as chiral selectors on silica.

Keywords: Peak shape; Non-linear chromatography; Mass transfer; Adsorption isotherms; Kinetic studies

1. Introduction

Peak tailing is an ubiquitous plague in analytical applications of chromatography. It has been blamed on many processes taking place inside or outside the column. It has become relatively easy to find out and remediate to outside sources of tailing (e.g., tailing injection, slow detector response). Accordingly, extra-column sources of tailing have become a less important contribution with modern instruments. Still, peak tailing is a serious practical problem and a vexing theoretical problem. All models of linear chromatography predict Gaussian peak profiles unless the column efficiency is very poor, well below

*Corresponding author. Address for correspondence: Department of Chemistry, University of Tennessee, 575 Buehler Hall, Knoxville, TN 37996-1600, USA.

[1]Permanent address: Analytical Pharmaceutical Chemistry, Uppsala University BMC, Box 574, S-751 23 Uppsala, Sweden.

0021-9673/96/$15.00
PII S0021-9673(96)00323-8

100 theoretical plates [1]. A considerable amount of purely empirical modeling work has been done in attempts to account for peak tailing in linear chromatography [2]. Unfortunately, these modeling efforts have left obscure the causes for peak tailing and failed to provide any meaningful remediation.

Peak tailing at low, analytical-scale concentrations has been explained previously as a consequence of the heterogeneity of the stationary phase [3]. A simple model of the phenomenon assumes an adsorbent whose surface is covered with a large proportion of low-energy adsorption sites, which are nonselective and involve dispersive or simple polar interactions and a small proportion of high-energy adsorption sites, which involve selective or specific interactions, including the formation of hydrogen bonding interactions or outer-shell complexation [3,4]. One of the difficulties encountered in the development of this theoretical model is the lack of authentic surfaces with a well-defined surface composition. If the surface composition cannot be controlled and the two types of sites studied separately, the values of the parameters have to be derived by identification of actual experimental results and numerical solutions of the model. With a sufficient number of parameters, agreement between the profiles of experimental and theoretical origin proves nothing and we are not better off than with the purely empirical approaches.

Chiral phases, however, provide an excellent system for this kind of studies. First, they are designed as two-types-of-sites surfaces. They contain highly selective sites which give strong interactions with at least one of the two enantiomers. These interactions involve usually the formation of two hydrogen bonds and a third, weaker, interaction in a steric pattern fitting better one of the enantiomers than the other. The density of these sites on the surface of the phase is rather low, leading to a value of the saturation capacity which is much lower than for the nonselective sites. Because the selective interaction is strong, the mass transfer kinetics on these sites tends to be slow. Finally, if the adsorption energy is high and the saturation capacity of the selective sites low, the retention on the selective sites is comparable to that on the nonselective sites. The equilibrium isotherms of each component is the sum of two terms accounting for its adsorption on each type of sites. Usually, each of the two terms are well approximated by a Langmuir model. The one for the selective sites because they are few, hence remote from each other. So, adsorbate–adsorbate interactions are reduced or nonexistent. Because the adsorption energy on the active sites is high, these sites are practically saturated at low concentrations in the liquid phase. Accordingly, the activity coefficients of the solutes remain close to 1 and the adsorption isotherm on the general type of sites is also well approximated by a Langmuir model.

This model is well suited to account for the interactions of enantiomers on the protein selectors used in chiral chromatography [5,6]. It is also convenient to account for band profiles observed in conventional reversed-phase liquid chromatography, using *n*-octadecyl silica as a stationary phase to separate hydrophobic drugs having polar amine functions [7,8]. Even at low concentrations, in a range where linear behavior is observed for simpler analytes and where a similar behavior is expected, peak tailing occurs for these compounds. In such cases, the concentrations, although small enough to cause the general type of sites to operate under linear conditions, are often sufficiently high to cause the selective type of sites to operate under nonlinear conditions. Then, the band profiles result from a combination of heterogeneous kinetics, heterogeneous thermodynamics and concentration overload of at least one type of adsorption sites. Note that, although adsorption has been taken as an example in the following, most explanations would be valid as well for other retention mechanisms, provided the appropriate changes are made.

It has been demonstrated earlier [1,9] that homogenous mass transfer kinetics cannot explain peak tailing in the linear case, unless the column efficiency does not exceed a few theoretical plates. This result is derived simply, by calculating band profiles with the transport–dispersive model. It is in agreement with the early results obtained by Giddings with a stochastic model [3,4,10]. Recently, however, it was shown that the use of the transport–dispersive model with the model of the two-kind-of-sites surface described above allows the calculation of narrow peaks, corresponding to a high column efficiency, but with a significant amount of tailing around the peak base [9]. Such profiles are obtained

even for a linear isotherm, provided that the rate of mass transfer kinetics are different on each type of sites. Severe peak tailing was demonstrated when the mass transfer coefficient of the second type of sites was 20 to 2000 times slower than that of the first type of sites. The smaller the contribution of this type of site to the retention of the compound, the closer the peak profile approaches an L-shape, with a narrow, high band having a long, low tail [9]. This kind of peak tailing is difficult to eliminate since a small degree of tailing still remains when the value of the initial slope of the contribution of these adsorption sites to the global isotherm is more than 1000 times smaller than that of the first type of adsorption sites (i.e., with $a_1/a_2 \geq 1000$).

The purpose of the present work is an investigation of the combined effects of two sources of peak tailing: (1) an heterogeneous kinetics, the higher adsorption- energy sites having a slow mass transfer kinetics and (2) the operation of these sites under nonlinear conditions. We detail the separate effects first, then discuss their combination, using systematic computer calculations of band profiles based upon the transport–dispersive model, a modified solid film linear driving force (LDF) model accounting for the mass transfer kinetics on each types of sites, and a bi-Langmuir isotherm. In a further work, we will show that the transport–dispersive model with partial overload can be used to explain the origin of the severe tailing of the profiles of β-blockers enantiomers on some chiral phases [11].

In the following, we call sites of type I those with which the molecular interactions of the analytes involve only dispersive or simple polar forces of moderate energy and limited selectivity. On these type I sites, the mass transfer kinetics is fast. We call sites of type II those with which analyte molecules undergo strong, highly selective interactions. On these sites, the mass transfer kinetics tends to be slow. We assume that both the type I and the type II surface are homogeneous.

2. Theory

The transport–dispersive model was used for systematic calculations of band profiles. In this lumped kinetic model, the mass transfer kinetics is represented by the equation of the solid film linear driving force model. Since we assume a heterogeneous surface with two types of sites, we need two such equations, with different rate constants. Similarly, the adsorption isotherm on each site is accounted for by the Langmuir model. Thus, the global isotherm is given by the bilangmuir isotherm.

2.1. Column model

The mass balance equation for the transport–dispersive model is

$$u\frac{\partial C}{\partial z}+\frac{\partial C}{\partial t}+F\frac{\partial q}{\partial t}=D\frac{\partial^2 C}{\partial z^2} \tag{1}$$

where t and z are the time and axial positions in the column, respectively, C and q are the local concentrations in the mobile and stationary phase, respectively, u is the mobile phase velocity, F is the phase ratio and D is the axial dispersion coefficient.

The initial condition characterizes the state of the column when the injection is performed. This corresponds to a column empty of sample and containing only mobile and stationary phase in equilibrium

$$C(t=0, z)=0 \tag{2}$$

The classical boundary conditions of nonlinear chromatography were used, assuming a rectangular injection pulse with a width t_p and a maximum concentration C^0 at the column inlet as follows

$$C(t, z=0)=C^0 \qquad 0 \leq t \leq t_p \tag{3a}$$

$$C(t, z=0)=0 \qquad t<0 \vee t>t_p \tag{3b}$$

2.2. Equilibrium isotherms

The isotherm equation relates the concentration of a component in the mobile phase and its concentration in the stationary phase at constant temperature. In many simple achiral separations done in chromatography, the Langmuir isotherm equation [12] accounts well for the adsorption of a single component on a homogeneous surface.

$$q^*=\frac{aC}{1+bC} \tag{4}$$

where q^* is the stationary phase concentration at equilibrium with the mobile phase concentration C, a is the initial slope of the isotherm and b is a term related to the adsorption energy; a/b is q_s, the monolayer capacity.

In this work, we consider that the surface of the adsorbent has two different types of adsorption sites. The simplest isotherm model consistent with the surface model assumed in this work is the bi-Langmuir isotherm [12]. This model has been used successfully to describe the adsorption equilibrium behavior of enantiomeric pairs on various chiral stationary phases. The equation is

$$q^* = q^*_1 + q^*_2 = \frac{a_1 C}{1 + b_1 C} + \frac{a_2 C}{1 + b_2 C} \quad (5)$$

In this equation, the numerical coefficients a_1 and b_1 correspond to the type-I adsorption sites. In enantiomeric separations, these coefficients are the same for the two optical isomers. The coefficients a_2 and b_2 correspond to type-II sites. a_1/b_1 is the monolayer capacity for type-I sites, $q_{1,s}$ and a_2/b_2 is the monolayer capacity for type-II sites, $q_{2,s}$. Usually b_2 is much larger than b_1 and $q_{2,s}$ much smaller than $q_{1,s}$. a_1 and a_2 are often of comparable magnitude, although a_2 is often smaller than a_1. In enantiomeric separations, a_2 and b_2 are different for the two enantiomers.

2.3. Kinetics of mass transfer

A solid film linear driving force (LDF) model was used to account for the mass transfer kinetics on each of the two types of sites [9]. This leads to the following set of equations

$$\frac{\partial q_1}{\partial t} = k_1(q^*_1 - q_1) \quad (6)$$

$$\frac{\partial q_2}{\partial t} = k_2(q^*_2 - q_2) \quad (7)$$

$$q = q_1 + q_2 \quad (8)$$

where q^*_1 is the stationary phase concentration in equilibrium with the mobile phase concentration C_i (i.e., $q^*_1 = a_i C_i$). The peak tailing is assumed to originate from a slow desorption rate of the type-II sites (i.e., $k_2 \ll k_1$). These sites have, generally, a higher adsorption energy, hence a longer average residence time than the nonselective sites.

The system of Eqs. (1–8) can be solved numerically by using the backward-forward finite difference method [9]. When necessary, the degree of asymmetry of the bands is quantified by calculating the asymmetry factor, or ratio of the second or left part of the peak over the first or early part of the peak at 10% of the peak height [9].

3. Results and discussion

This study is focused on the influence of a slow kinetics of adsorption- desorption at type-II sites, under linear and nonlinear conditions concerning type-II sites and under linear conditions concerning type-I sites. Parameters hold constant are the column length (10 cm), the flow velocity (6.02 cm/min, i.e., 0.80 ml/min in a 4.6 mm I.D. column), the injection time, t_p, (0.02 min), and the total packing porosity, ($\epsilon = 0.8$), hence the phase ratio, F (0.25). Thus, the hold-up time, t_0, was 1.66 min. The injected concentration, C^0, was 0.1 mM.

Since we are interested only in nonlinear conditions concerning the type-II sites and we want the type-I sites to operate under linear conditions, the isotherm parameters were hold constant at $a_1 = 10$ and $b_1 = 0.20$ mM^{-1}. This allows for linear conditions because $b_1 C$ is equal to 0.02 and the loading factor for type-I sites is $L_{f,1} = 0.01\%$ [1]. Although, there is no distinct borderline between linear and nonlinear conditions, linearity can be assumed when those two factors have values lower than 0.05.

The loading factor is given by

$$L_f = \frac{T_p C^0}{t_0 F q_s} \quad (9)$$

The present study aims at elucidating the separate and combined influence on the band profiles of the values of the mass transfer coefficients for type-I and type-II adsorption sites, k_1 and k_2, and of the thermodynamic parameters for type-II sites, a_2 and b_2. First, the effects of a slow rate of mass transfer for type-I sites was investigated. After this part of the study had been completed, k_1 was kept constant at a very high value, $k_1 = 10\,000$ min^{-1}; a_2 was varied from 10.0 to 0.01; b_2 was set either to 0 or to a very high value, 10 or 20 mM^{-1}, ensuring the isotherm of type-II sites to be either linear ($b_2 = 0$) or

nonlinear ($b_2 = 10$ or 20), respectively, for the concentrations used. Increasing the degree of nonlinear behavior by increasing the value of b_2 at constant value of a_2 results in a simultaneous decrease of $q_{s,2}$ (cf. Eq. 5). Thus, $L_{f,2}$ increased with increasing b_2C. High values for both $L_{f,2}$ and b_2 ensure nonlinear, overloaded behavior for adsorption on type-II sites; k_2 was varied from 0.1 to 10 000 min^{-1}. The influence of axial dispersion has a dampening effect on the peak tailing due to heterogenous thermodynamics, as shown previously [9]. This effect was entirely neglected in this work and D was set to 0 in Eq. (1). The chromatograms are given as profiles of the concentration (mM) versus the retention factor, $k' = (t - t_0)/t_0$.

3.1. Homogenous mass transfer kinetics under nonlinear conditions, for a two-site adsorption model, $a_1 \neq a_2$

We illustrate first, for further reference, the case when we have adsorption on a two-types of sites surface, with homogenous kinetics behavior, and when the rate constant of this kinetics increases from an extremely low value to near infinitely fast kinetics. As a reference, the profiles obtained in the linear case are shown in Fig. 1. In this case, the value of b_2 was 0, to ensure linear behavior of both isotherm terms. The following values of $k_1 = k_2$ were selected (1)[2] 0.1; (2) 0.3; (3) 1.0; (4) 10; (5) 100; (6) 1000; and (7) 10 000 min^{-1}. At the lowest value of the rate constant ($k_1 = k_2 = 0.1$ min^{-1}, peak 1), the peak behaves as if it were unretained. When the value of the rate constant increases, a long tail on an unretained peak is formed first ($k_1 = k_2 = 0.3$ min^{-1}, peak 2); then, the initial sharp peak disappears and the tail becomes a broad band ($k_1 = k_2 = 1.0$ min^{-1}, peak 3) which narrows progressively and turns first into a distinct, albeit very broad peak ($k_1 = k_2 = 10.0$ min^{-1}, peak 4); and then into an actual peak whose efficiency increases with increasing rate constant ($k_1 = k_2 = 100.0$ to 10 000 min^{-1}, peaks 5–7, respectively). Note that when the rate coefficient increases beyond ca. 100 min^{-1} (peaks 5–7), the peaks are

[2]Reference number of the peak in parentheses.

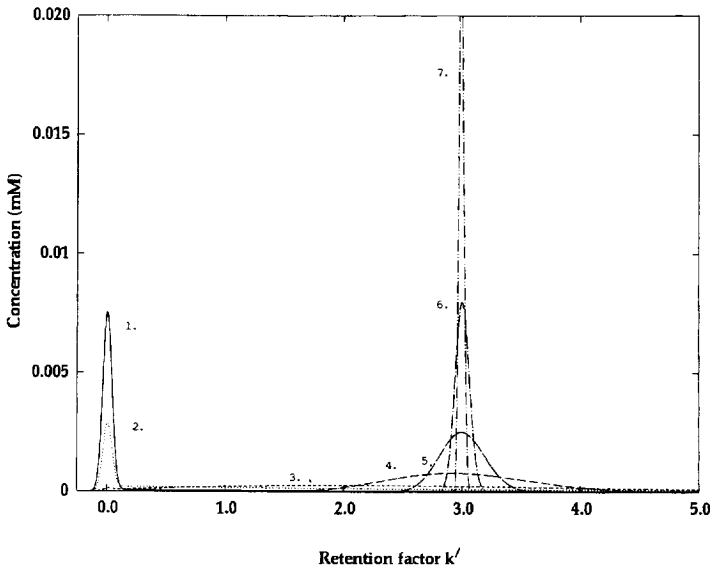

Fig. 1. Peak profiles calculated under linear conditions, using the transport–dispersive model, assuming bi-Langmuir adsorption behavior and identical mass transfer coefficients. The axial dispersion coefficient (Eq. 1) is 0, so the column efficiency is controlled by the mass transfer kinetics. The column length was 10 cm, the linear velocity 6.02 cm/min, the injection time 0.02 min and the total packing porosity 0.800. Langmuir coefficients (Eq. 5): $a_1 = 10.0$; $a_2 = 2.0$; $b_1 = 0.20$ mM^{-1} (giving linear behavior for type-I sites, with ($b_1C = 0.02$ and $L_{f,1} = 0.01\%$); and $b_2 = 0$ (giving true linear conditions for type-II sites. Sample concentration, 0.1 mM. Mass transfer kinetics coefficients ($k_1 = k_2$), in min^{-1}: peak 1, 0.1; peak 2, 0.3; peak 3, 1; peak 4, 10; peak 5, 100; peak 6, 1000; peak 7, 10 000.

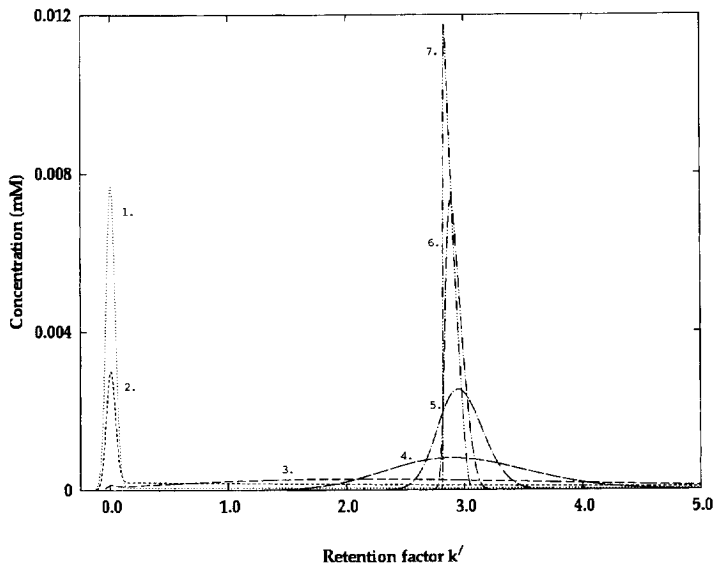

Fig. 2. Same as Fig. 1, but $b_2 = 20$ mM^{-1}. This gives strongly overloaded behavior to type-II sites under the experimental conditions selected ($b_2C = 2.0$ and $L_{f,2} = 4.82\%$). Peak asymmetry factor (at 10% of peak height): (4), 1.25 ($k_1 = 10$); (5), 1.19 ($k_1 = 100$); (6), 2.21 ($k_1 = 1000$); (7), 9.1 ($k_1 = 10\,000$).

symmetrical and their retention time becomes constant.

Fig. 2 shows similar results obtained with a different second term of the global isotherm, now strongly nonlinear, with $b_2 = 20$ mM^{-1}. Under these conditions, $b_2C = 2.0$ and $L_{f,2} = 4.8\%$. The peaks or bands 1 to 4 have nearly the same shapes as in Fig. 1. When the mass transfer coefficient increases beyond a relatively high value (ca. 50 min^{-1}), the bands become unsymmetrical and their retention time decreases with increasing rate constant [13]. At $k_1 = k_2 = 100.0$ to 10 000 min^{-1} (peaks 5–7), the nonlinear behavior is obvious. It becomes stronger and stronger with increasing value of the rate constant. So, while in Fig. 1 there is tailing only for very low values of the rate constant (homogeneous kinetics tailing), in Fig. 2 there is peak tailing both at low values of the rate constant (homogeneous kinetics tailing) and at high values of the rate constant (overloaded band peak tailing). This tailing is due to the overloading of type-II adsorption sites. It takes place at medium fast or fast mass transfer kinetics. The variation of the asymmetry factor illustrates the point. At low values of the rate constant, the peak is unsymmetrical for kinetics reasons and becomes less and less so when the rate coefficient increases. At high values of the rate constant, the peak is unsymmetrical for thermodynamics reason: it is narrow and high. Its maximum samples regions of high concentrations where the isotherm is strongly nonlinear. The degree of asymmetry increases with increasing value of the rate constant because the peak is higher and less disperse.

This result is the same as the one obtained previously in the case of homogeneous thermodynamics, i.e., in the simple Langmuir case [1,13,14]. It provides a useful starting point for an investigation of peak tailing originating from heterogenous mass transfer kinetics combined with a nonlinear behavior of the phase equilibrium, as discussed below.

3.2. Heterogenous mass transfer kinetics under nonlinear conditions for the sites of the second type

3.2.1. Overview over extreme kinetic conditions

Interesting new features appears in the chromatograms when we investigate the influence of heterogenous mass transfer kinetics. The discussion of the various peak profiles obtained under the combined influence of a nonlinear isotherm and a slow mass transfer kinetics for the second type of

adsorption sites is complicated. To illustrate its nature and its importance, we show first peaks obtained under different and extreme kinetic conditions, with very fast and very slow mass transfer kinetics at either one or both of the two types of adsorption sites, and under nonlinear adsorption behavior at site 2.

Fig. 3 illustrates these kinetics effects for $a_2=2$ and $b_2=20$ mM^{-1}. The figure shows four different peaks. For peaks 1 to 4, the values of the mass transfer coefficients were $k_1=k_2=0.1$ min^{-1} for peak 1, $k_1=0.1$ and $k_2=10\,000$ for peak 2, $k_1=10\,000$ and $k_2=0.1$ for peak 3 and $k_1=k_2=10\,000$ min^{-1} for peak 4. For the first peak there is no retention at all since mass transfer kinetics is too slow at both types of sites. For peak 2, near equilibrium is achieved on type-II adsorption sites, but still the retention contribution of type-I sites is negligible. The peak tails because of the high degree of nonlinear behavior on type-II sites. For peak 3, the converse is true. The only retention contribution in this case originates from type-I adsorption sites. Since these sites operate under linear conditions, the peak has a Gaussian shape and exhibits no tailing. For peak 4, both adsorption sites operate near equilibrium. However, the peak exhibits a significant degree of tailing because type-II sites are strongly overloaded.

3.2.2. *Influence of the rate constant on type-I sites at constant rate on type-II sites*

This situation was also previously discussed in the linear case [9]. We now extends the discussion to the nonlinear case. In Fig. 4a and Fig. 4b, the value of a_2 was 2 ($a_1=10$) and the value of the mass transfer kinetics for type-II adsorption sites was hold constant, at a value corresponding to relatively slow mass transfers, $k_2=10$ min^{-1}. By contrast, the mass transfer rate constant for type-I sites was varied in a broad range. k_1 was set at the following values, for peak 1, 0.1 min^{-1}; for peak 2, 1.0; for peak 3, 10; for peak 4, 100; for peak 5, 1000; and for peak 6, 10 000 min^{-1}. In Fig. 4a, the isotherm of type-II sites is linear ($b_2=0$). As previously concluded [9], all peaks exhibits tailing. The most interesting case is when the mass transfer kinetics becomes very fast on type-I sites, which then operate near equilibrium (peaks 5 and 6). Important peak tailing takes place because of having heterogenous mass transfer kinetics. The increase of the asymmetry factor with increasing rate constant for type-I sites illustrates this

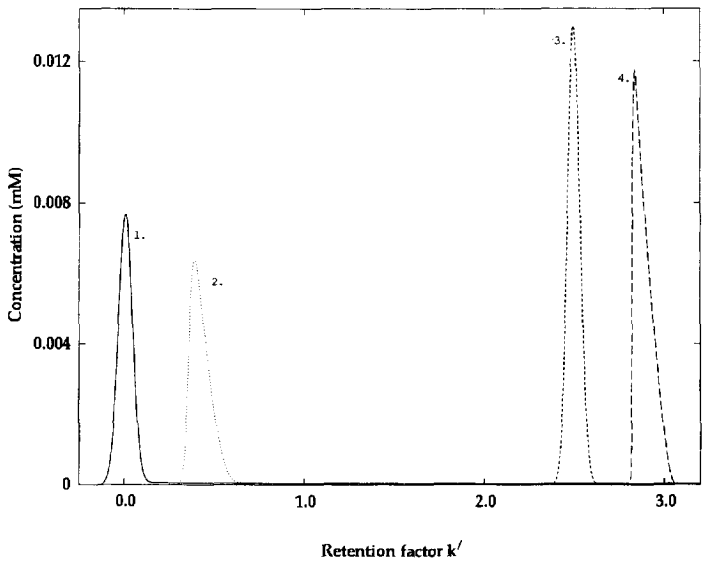

Fig. 3. Same as Fig. 2, but the profiles were calculated for widely different combinations of the values of the rate constant of mass transfer kinetics: peak 1, $k_1=k_2=0.1$ min^{-1}; peak 2, $k_1=0.1$ and $k_2=10\,000$ min^{-1}; peak 3, $k_1=10\,000$ and $k_2=0.1$ min^{-1}; peak 4, $k_1=k_2=10\,000$ min^{-1} ($a_1=10$ and $a_2=2$).

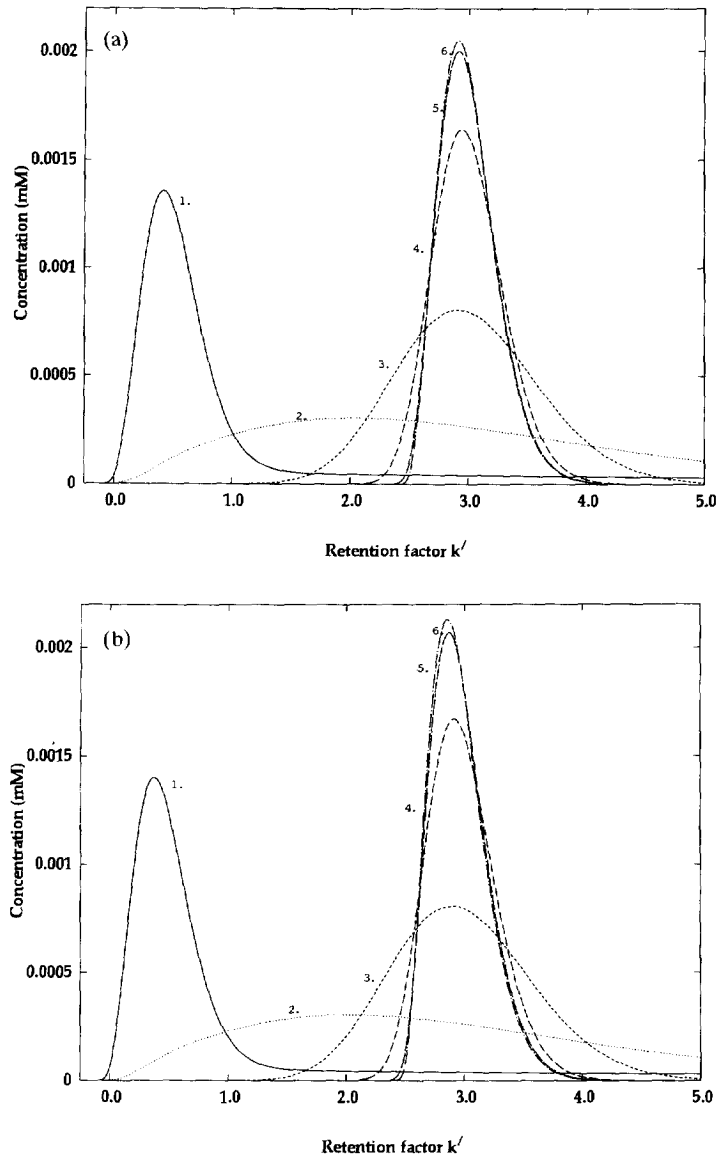

Fig. 4. Same as Fig. 1 with slow mass transfer kinetics on type-II sites ($k_2 = 10.0$ min^{-1}). Rate constant k_1: for peak 1, 0.1; for peak 2, 1.0; for peak 3, 10; for peak 4, 100; for peak 5, 1000; for peak 6, 10 000 min^{-1}. (a) $b_2 = 0$. Peak asymmetry factors (at 10% of peak height), peaks 3, 1.24; 4, 1.36; 5, 1.71; 6, 1.81. (b) $b_2 = 20$ mM^{-1}. Peak asymmetry factors (at 10% of peak height), peaks 3, 1.26; 4, 1.42; 5, 1.89; 6, 2.02.

phenomenon (Fig. 4a). For peak 3, the kinetics is slow, the rate constant equal for both types of sites, and the asymmetry factor is 1.24. The tailing is due to the slow mass transfer kinetics [9]. For peak 4, the rate constant on type-I sites is increased ten-fold and the tailing increases [asymmetry factor (asf) = 1.36]. This effect is enhanced with peaks 5 (asf = 1.71) and 6 (asf = 1.81) for which the rate constant on type-I sites is 100 and 1000 times faster than on type-II sites. The apparent efficiency is limited in this case, because of the moderate value of the ratio a_1/a_2. It would become very large if the ratio a_1/a_2 would be

larger instead of being merely 5 as it is in Fig. 4 [9]. In the present case, however, the peak tailing originates entirely in the heterogeneous mass transfer kinetics.

The nonlinear case is illustrated in Fig. 4b. The isotherm of the type-II sites has a low saturation capacity, with $b_2 = 20$ mM^{-1}. The nonlinear behavior should be severe, with $b_2C = 2.0$ and a value of the loading factor for type-II sites, $L_{f,2} = 4.8\%$. At first glance, however, there are almost no differences between Fig. 4a and Fig. 4b. Almost all the peak tailing seems to originate only from the slow kinetics of mass transfer on type-II sites, with a negligible contribution coming from nonlinear behavior. The influence on the band profiles of the overloading of type-II sites appears to be drowned in the tailing of these bands due to the slow mass transfer on these very sites. However, the variation of the asymmetry factor with increasing rate constant on type-I sites and the difference between the value of this factor for corresponding peaks in Fig. 4a and Fig. 4b reveals the strong influence of the rate constant but also a small influence of the nonlinear behavior of the isotherm. The asymmetry factor increases with increasing rate constant of mass transfer on the retention-dominating type-I sites, because of the severe overloading of type-II sites. For peaks 3 to 6 in Fig. 4b, the values of the asf are respectively, 1.26, 1.42, 1.89, and 2.02. The difference is small but not negligible. Further investigation is required.

3.2.3. Very fast kinetics for type-I sites and slow kinetics on type-II sites

Thus, fast mass transfer was assumed on type-I sites by holding k_1 constant at 10 000 min^{-1}, while the rate constant of the mass transfer kinetics on type-II sites was decreased to $k_2 = 1.0$ min^{-1}, a relatively low value. At the same time, the saturation capacity for these sites was changed. This amounts to changing the degree of overload of these sites at constant sample size by changing b_2. In Fig. 5a, the three peak profiles correspond to $b_2 = 0$ for peak 1, 10 mM^{-1} for peak 2 and 20 mM^{-1} for peak 3. The severe overloading of the type-II sites under these conditions, due to the considerable increase of the b_2 value, has no impact on the strongly unsymmetrical, very narrow peak, with a long tail. As explained previously [9], this strange L-shaped tail, observed when the rate of the mass transfer kinetics on the type-II sites is low. At $k = 0.1$ min^{-1}, this contribution disappears completely (cf. Fig. 1, peak 1). This result suggests that the influence of a nonlinear isotherm on the band profile is significant only when the mass transfer rate constant is high. If mass transfers are slow on type-II sites, their kinetics controls the band profiles.

This is illustrated in Fig. 5b–e. The rate constant of the mass transfer kinetics on type-II sites was increased at constant values of the other parameters, with k_2 values of 10, 50, 100 and 10 000 min^{-1} for Fig. 5b, Fig. 5c, Fig. 5d and Fig. 5e, respectively. Peak 1 (linear isotherm) exhibits a tailing due to heterogeneous kinetics at low value of the rate constant, k_2 (Fig. 5b and Fig. 5c). It becomes symmetrical for k_2 larger than ca. 50 min^{-1}. By contrast, the other two peaks become more unsymmetrical when the rate constant for the type-II sites increases. A steep front and a langmuirian tail can already be noticed in Fig. 5d and become typical of band overloading in Fig. 5e. The profiles obtained are similar to that of peak 6 in Fig. 4b, for which the mass transfer coefficient, k_2, was 10.

The consequences of this situation is that when there are type-II sites in the stationary phase, there is always band tailing if these type-II sites are overloaded and if mass transfer on these sites are significantly slower than on type-I sites, although the origin of this peak tailing is different at fast and slow mass transfer kinetics on type-II sites. If heterogeneous mass transfer on type-II sites (Fig. 5a) are slow, with or without overloading of a nonlinear isotherm on these sites, there is peak tailing of heterogeneous kinetics origin. If the mass transfer kinetics on type-II sites is fast, i.e., if $k_2 > 100$, peak tailing is caused by the heterogenous thermodynamics and the overload of these type-II sites (cf. Fig. 5d and Fig. 5e). Finally, there is an intermediate region, when k_2 is between 10 and 100 min^{-1}, in which peak tailing has a combined origin (cf. Fig. 5b and Fig. 5c).

It has been shown previously that in the linear case, heterogeneous mass transfer kinetics gives rise to an unsymmetrical, L-shaped peak with a significant tail even when the contribution of type-II sites to the retention, i.e., the value of a_2, is small. The

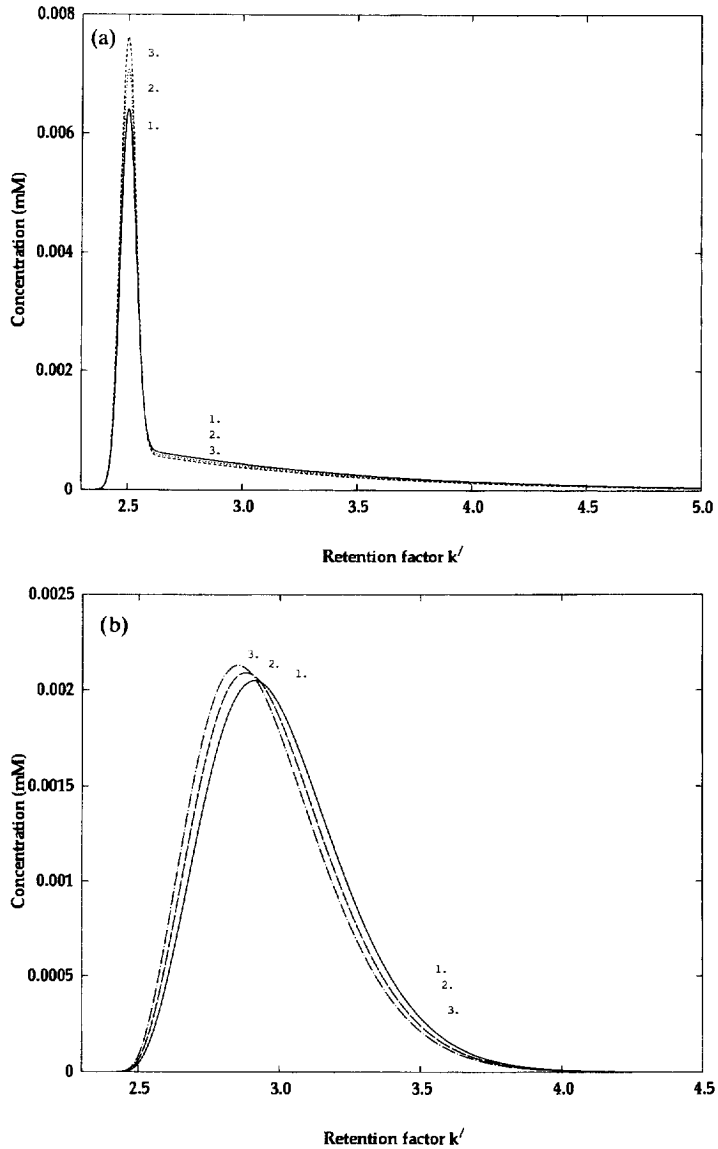

Fig. 5. Same as Fig. 1 ($a_1 = 10$ and $a_2 = 2$), with k_1 hold constant at 10 000 min^{-1}. The value of b_2 are 0 for the peaks 1, 10 mM^{-1} for the peaks 2, and 20 mM^{-1} for the peaks 3. (a) $k_2 = 1.0$ min^{-1}, (b) $k_2 = 10$ min^{-1}, (c) $k_2 = 50$ min^{-1}, (d) $k_2 = 100$ min^{-1}, (e) $k_2 = 10\,000$ min^{-1}.

tail of this L-shaped peak was found to be important even at values of $a_1/a_2 > 1000$. Thus, a comprehensive study of peak tailing must include the case in which this tailing is due to the overloading of type-II sites when the mass transfer kinetics on both types of sites is extremely fast (pure heterogeneous thermodynamics). Peak 4 in Fig. 3 was a first example of this case. Fig. 6 illustrates the influence of heterogeneous thermodynamics on peak tailing at fast mass transfer kinetics on both sites. The value used for the rate constant in the calculations is $k_1 = k_2 = 10\,000$ min^{-1}, and b_2 was set at 20 mM^{-1}. The a_2 values are 2.0 for peak 1; 1.0 for peak 2; 0.1 for peak 3; 0.04 for peak 4; 0.01 for peak 5 and 0.0 for peak 6. Thus, peak 6 is a reference peak. The decrease of the value of a_2 from peak 1 to peak 5 causes the loading

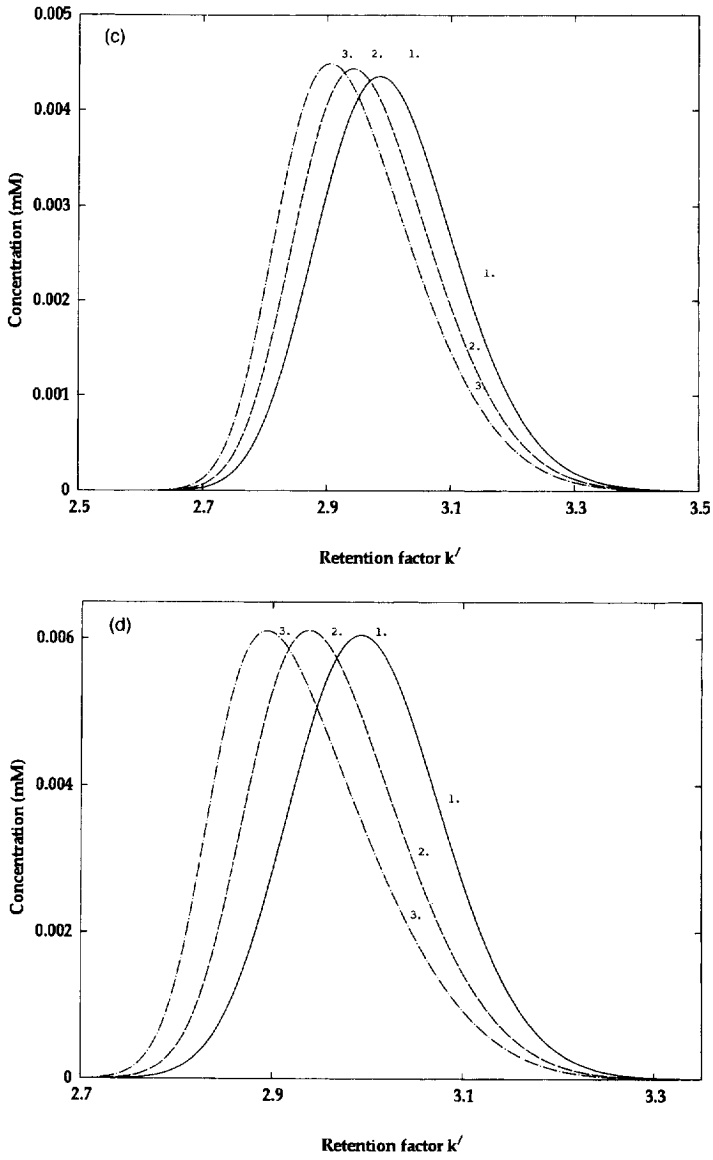

Fig. 5. (*continued*)

factor for type-II sites to increase considerably, from $L_{f,2}=4.8\%$ for peak 1 to values well above 100% for peaks 3 to 5. When a_2 becomes smaller and smaller, the contribution to the peak shape caused by the nonlinear behavior of the isotherm, i.e., the amount of peak tailing, decreases. The contribution of a nonlinear isotherm to peak tailing seems to have become negligible when a_2 becomes smaller than 0.1. This corresponds to a value of the ratio a_2/a_1 larger than 100. Fig. 6 shows also that the diffuse rear boundary of the peak is affected as a whole and not only at the peak base. Although the intensity of peak tailing due to the overloading of type-II sites decreases, the band keeps the same characteristic shape.

Finally, it is instructive to discuss the change in peak profile arising in connection with a decrease of the relative contribution of type-II sites to retention.

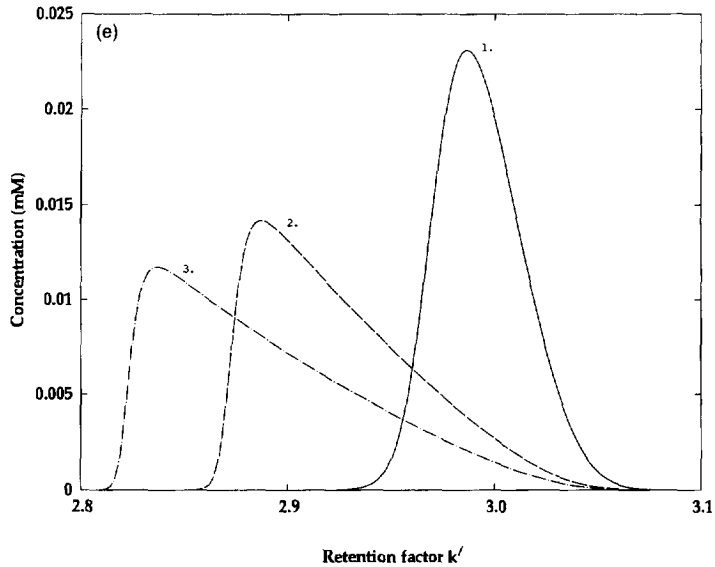

Fig. 5. (*continued*)

In the linear case, significant peak tailing is caused by heterogenous mass transfer kinetics at very low values of a_2/a_1, between 10^{-2} and 10^{-3}. We discuss now the influence on this tailing of isotherm overloading. Fig. 7 shows profiles calculated with small values of a_2, under linear and nonlinear conditions on type-II sites, for two different values of the rate constant, k_2, 10 (Fig. 7a) and 50 (Fig. 7b) min^{-1}. In

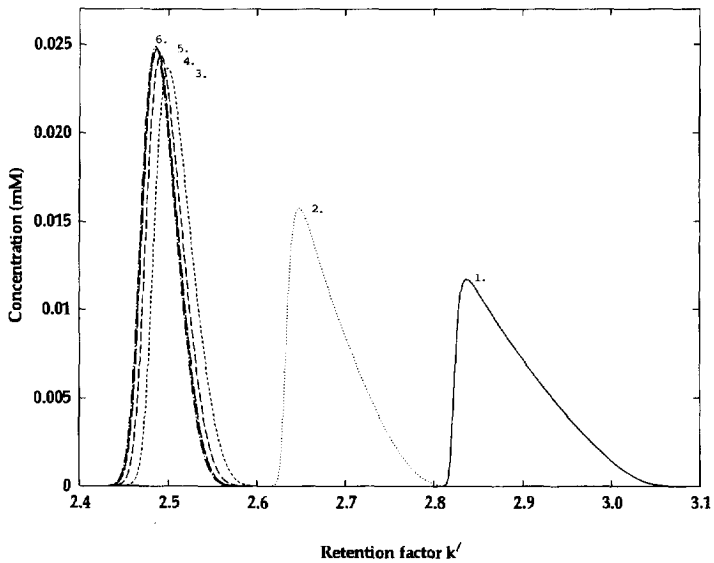

Fig. 6. Same as Fig. 1 but with small, different values of a_2, $k_1 = k_2 = 10\,000$ min^{-1} and $b_2 = 20$ mM^{-1} (except for peak 6, $b_2 = 0$). Values of a_2: for peak 1, 2.0; for peak 2, 1.0; for peak 3, 0.1; for peak 4, 0.04; for peak 5, 0.01; for peak 6, 0. Peak 6 is a reference (no type-II adsorption sites). For peaks 1–5, $b_2C = 2.0$ and $L_{1,2} = 4.8\%$ for peak 1; 9.6% for peak 2; and >100% for peaks 3 to 5.

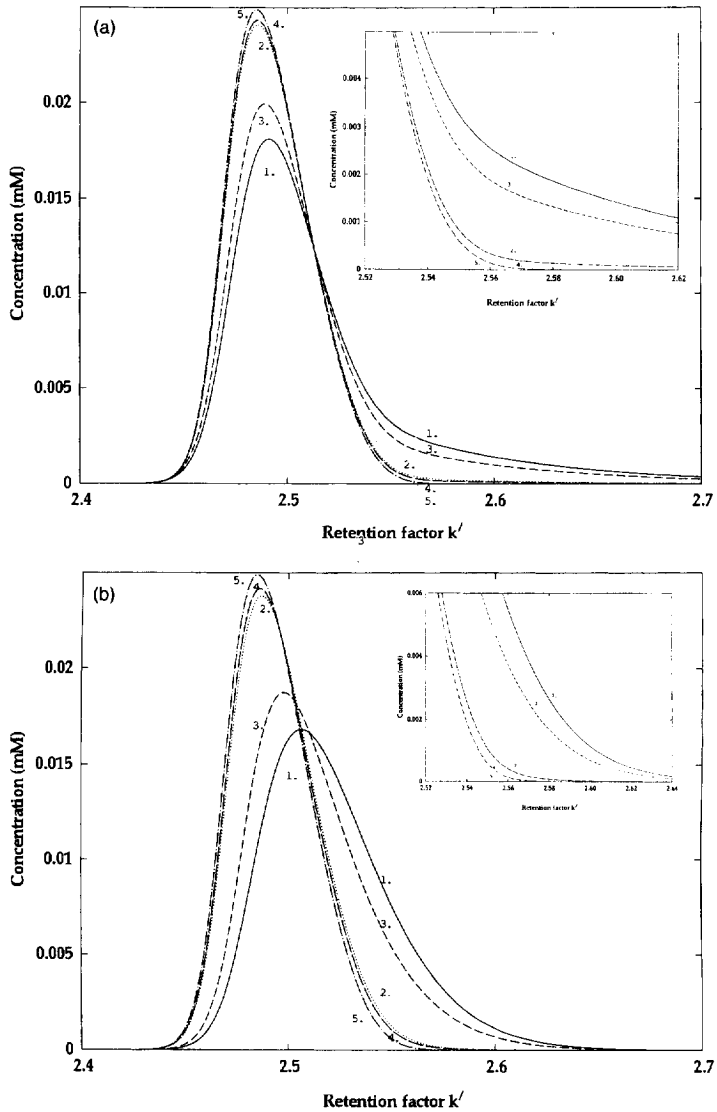

Fig. 7. Same as Fig. 6, except comparison of the profiles calculated with two small values of a_2 under linear and nonlinear conditions for type-II sites, with different rate constants of the mass transfer kinetics. Values of a_2: 0.1 for peaks 1 and 3; 0.01 for peaks 2 and 4. Values of b_2: 0 for peaks 1 and 2; 20 mM^{-1} for peaks 3 and 4. Peak 5 is a reference peak (no type-II sites). (a) $k_2 = 10$ min^{-1}; (b) $k_2 = 50$ min^{-1}.

both Fig. 7a and Fig. 7b, the value of a_2 is 0.1 for peaks 1 and 3 ($a_1/a_2 = 100$); 0.01 for peaks 2 and 4 ($a_1/a_2 = 1000$) and 0 for peak 5 (no type-II sites). The value of b_2 is 0 for peaks 1 and 2 and 20 000 for peaks 3 and 4. Peak 5 is used as a reference. The inset of each figure shows the peak tails on a larger scale. In both figures, the smaller the contribution to the retention of type-II sites, the less important the area of the peak tail. This area is also less important when the mass transfer kinetics is slower (Fig. 7a and Fig. 7b). The mass transfer rate constant is small in Fig. 7a ($k_2 = 10.0$ min^{-1}) and moderate in Fig. 7b ($k_2 = 50$ min^{-1}). Comparing peaks 1 and 3 on the one hand, peaks 2 and 4 on the other shows that column overloading tends to decrease the relative importance of the L-shaped peak tailing and that it

does so more when the mass transfer rate constant increases.

4. Conclusion

A major cause of peak tailing in analytical scale separations is due to the existence of two types of adsorption sites, the second type of sites covering a small fraction of the surface area, contributing moderately to the retention, having a small saturation capacity and relatively slow mass transfer kinetics. When the mass transfer kinetics on the type-II sites is very slow, peak tailing arises only from this kinetic origin. At fast mass transfer kinetics, it has only a thermodynamic origin. In the intermediate region, for values of k_2 between 10 and 100 min^{-1}, peak tailing results from a combination of both sources in a complex interplay. Peak tailing of kinetic origin is important even at values of a_1/a_2 of the order of 1000 whereas the tailing of thermodynamic origin becomes negligible when a_1/a_2 becomes larger than 100. When $a_1/a_2 > 100$, peak tailing is always entirely of kinetic origin. Therefore, it is important to eliminate entirely the type-II adsorption sites, even if their contribution to the retention is negligible. This is especially important in analyses performed for purity control of compounds such as the active ingredients of drugs. In such cases, large size samples are injected in the column and low concentration impurities may be hidden in the long, L-shaped tail of the main component under conditions which cause significant tailing of this compound.

In most cases, the type-II site isotherm is much more strongly curved than the isotherm of type-I sites; b_2 is much larger than b_1 and $q_{s,2}$ is much smaller than $q_{s,1}$. In the case in point earlier, the ratio b_2/b_1 was equal to 100. Because $a_2/a_1 = b_2\ q_{s,2}\ /\ (b_1\ q_{s,1})$, the reduction of the relative contribution of the type-II sites, a_2/a_1, below 10^{-3} may require the reduction of the relative monolayer saturation capacity, i.e., in practice the density of surface coverage by these type-II sites, to around 1 ppm or even lower.

As we show in a forthcoming publication [11], the present study provides a most satisfactory explanation of the phenomenon of peak tailing in many systems used to perform analytical separations and of the influence of the experimental conditions on the degree of tailing. This is especially relevant in the case of chiral separations when the mass transfer kinetics is slow or moderately fast (e.g., for β-blocker drugs analyzed on cellulase proteins as chiral selectors).

Acknowledgments

This work was supported in part by grant CHE-9201663 from the National Science Foundation and by the cooperative agreement between the University of Tennessee and the Oak Ridge National Laboratory. We acknowledge support of our computational effort by the University of Tennessee Computing Center. TF is grateful for the financial support awarded to him by Astra Hässle AB (Mölndal, Sweden) and by the Swedish Academy of Pharmaceutical Sciences (The Göran Schill Memorial Foundation).

References

[1] G. Guiochon, S. Golshan-Shirazi, and A.M. Katti, Fundamentals of Preparative and Nonlinear Chromatography, Academic Press, Boston, MA, 1994, Ch. VI.
[2] C.F. Poole and S.K. Poole, Chromatography Today, Elsevier, Amsterdam, 2nd ed., 1993.
[3] J.C. Giddings, Anal. Chem., 35 (1963) 1999.
[4] J.C. Giddings, Dynamics of Chromatography, Marcel Dekker, New York, 1965.
[5] S. Jacobson, S. Golshan-Shirazi and G. Guiochon, J. Am. Chem. Soc., 112 (1990) 6492.
[6] S. Jacobson, S. Golshan-Shirazi and G. Guiochon, J. Chromatogr., 522 (1990) 23.
[7] A. Sokolowski and K.-G. Wahlund, J. Chromatogr., 189 (1980) 299.
[8] T. Fornstedt and G. Guiochon, Anal. Chem., 66 (1994) 2686.
[9] T. Fornstedt, G. Zhong and G. Guiochon, J. Chromatogr. A, 741 (1996) 1.
[10] J.C. Giddings and H. Eyring, J. Phys. Chem., 59 (1955) 416
[11] T. Fornstedt, G. Zhong, Z. Bensetiti and G. Guiochon, Anal. Chem., in press.
[12] G. Guiochon, S.G. Shirazi and A.M. Katti, Fundamentals of Preparative and Nonlinear Chromatography, Academic Press, Boston, MA, 1994.
[13] B. Lin, S. Golshan-Shirazi and G. Guiochon, J. Phys. Chem., 93 (1989) 3363.
[14] B. Lin, T. Yun, G. Zhong and G. Guiochon, J. Chromatogr. A., 708 (1995) 1.